Journal of
Synchrotron
Radiation

ISSN 0909-0495

Received 15 February 2007
Accepted 26 March 2007

Application of glancing-emergent-angle fluorescence for polarized XAFS studies of single crystals

A. I. Frenkel,[a]* D. M. Pease,[b] J. I. Budnick,[b] P. Shanthakumar[b] and T. Huang[b]

[a]Department of Physics, Yeshiva University, New York, NY 10016, USA, and [b]Department of Physics, University of Connecticut, Storrs, CT 06269, USA. E-mail: frenkel@bnl.gov

X-ray absorption fine-structure (XAFS) data were obtained for the V *K*-edge for a series of anisotropic single crystals of $(Cr_xV_{1-x})_2O_3$. The data and the results were compared for the as-prepared bulk single crystals (measured in fluorescence in two different orientations) and those ground to powder (measured in transmission). For the bulk single crystals, the glancing-emergent-angle (GEA) method was used to minimize fluorescence distortion. The reliability of the GEA technique was tested by comparing the polarization-weighted single-crystal XAFS data with the experimental powder data. These data were found to be in excellent agreement throughout the entire energy range. Thus, it was possible to reliably measure individual V–V contributions parallel and perpendicular to the *c* axis of the single crystals, *i.e.* those unavailable by powder data XAFS analysis. These experiments demonstrate that GEA is a premiere method for non-destructive high-photon-count *in situ* studies of local structure in bulk single crystals.

© 2007 International Union of Crystallography
Printed in Singapore – all rights reserved

Keywords: X-ray absorption spectroscopy; fluorescence; single crystals; polarized measurements.

1. Introduction

Generally, the transmission method is considered to be the preferred method for XAFS data collection in the case of absorption edges of concentrated species. The counting statistics are better than those obtained in fluorescence, and, most importantly, fluorescence distortion (Goulon *et al.*, 1982) is absent in transmission data. Thus, most attempts to measure polarization-dependent data (by varying the angle between the X-ray polarization vector and the crystal axis) presently employ either elaborate sample preparation methods of transmission samples (Tranquada *et al.*, 1987; Haskel *et al.*, 1996, 2000), the measurement of thin films (that lack fluorescence distortion) in fluorescence (Woicik *et al.*, 1997; Nelson *et al.*, 2000; Kuykendall *et al.*, 2004) or application of analytical corrections that account for fluorescence distortion in the fluorescence mode of bulk single crystals (Tan *et al.*, 1981; Tröger *et al.*, 1992; Brewe *et al.*, 1994; Pfalzer *et al.*, 1999; Booth & Bridges, 2005). In this article we report results of our polarization-dependent XAFS measurements obtained for bulk single crystals of $(Cr_xV_{1-x})_2O_3$ for $x = 0$, 0.0116, 0.0285 and 0.0523. These materials have the corundum structure and exhibit a transition from metal (at $x < 0.01$) to insulator ($x > 0.01$), accompanied by a c/a ratio change (McWhan & Remeika, 1970). The mechanism of the transition is believed to be directly related to the change in the V–V distances both along the *c* axis and in the basal plane. However, the powder V *K*-edge XAFS is not helpful in resolving the two types of V–V distances and their change across the $x = 0.01$ Cr concentration. On the other hand, special techniques of sample preparation for transmission or fluorescence, described above, are not readily available for these and related materials with structural anisotropy where precise stoichiometry can be controlled by a specific synthetic route only. In this article we report the application of the glancing-emergent-angle (GEA) method of fluorescence measurements (Pease *et al.*, 1989; Suzuki, 1989) for polarization-dependent XAFS analysis.

2. Methods

Single crystals of $(Cr_xV_{1-x})_2O_3$ were made using the skull melting method, and characterized by resistivity measurements and energy-dispersive X-ray emission, as described previously (Metcalf & Honig, 1995). Characterization by X-ray powder diffraction revealed only the expected corundum structure peaks. Samples were aligned by means of a gas area detector diffractometer. XAFS data were obtained on the X-11A beamline of the National Synchrotron Light Source (NSLS). The samples were ground so that a flat parallel to the (110) plane was perpendicular to the incident beam. To find the $\mathbf{E} \parallel c$ and $\mathbf{E} \perp c$ orientations of the sample (where $\mathbf{E}$ is the electric field vector), we used the method

developed by Frenkel *et al.* (1997); namely we rotated the samples around the axis coaxial with the X-ray beam direction and XAFS scans were measured every 10°. For a perfect single-crystal,

$$\mu(\Theta) = \mu_{\parallel}\cos^2(\Theta) + \mu_{\perp}\sin^2(\Theta), \quad (1)$$

where $\mu_{\parallel}$ and $\mu_{\perp}$ are the energy-dependent absorption coefficients corresponding to $\Theta = 0°$ ($\mathbf{E}\parallel c$) and $\Theta = 90°$ ($\mathbf{E}\perp c$), respectively. Thus, using (1), we could find the angles corresponding to $\mu_{\parallel}$ and $\mu_{\perp}$. For each orientation, pure V foil was placed in front of the incident beam detector to align the data in absolute energy.

In the GEA mode, with normal incidence to the crystal flat and by blocking the beam to the ion chamber, we restricted the detected fluorescence to a small angle, which in our case was of the order 3° (Fig. 1). By such means, one simulates the fluorescence XAFS of a thin sample (Pease *et al.*, 1989). An additional advantage of the blocking shield was that it effectively blocked Bragg reflections from reaching the detector, the common obstacle in most fluorescence measurements of single crystals. The sample was mounted on a rotation stage for polarized measurements.

The fluorescence distortion, unless completely corrected for, manifests itself by a reduction in amplitude of the oscillatory portion of the signal in the extended XAFS (EXAFS) regime. Such sensitivity to the sample alignment allowed us to calibrate our procedure by comparing GEA data on single crystals with transmission on bulk powders obtained from the same samples. The GEA data were weighted as follows,

$$\mu_{\rm av} = \frac{1}{3}\mu_{\parallel} + \frac{2}{3}\mu_{\perp}. \quad (2)$$

This method of averaging simulates, from single-crystal data, the results expected for a random powder in transmission (Frenkel *et al.*, 1997). We then compared the XAFS from such 'simulated random powder' with results we obtained for actual ground powders of the same materials in transmission. We used the software package *IFEFFIT* (Newville, 2001) for data analysis and processing.

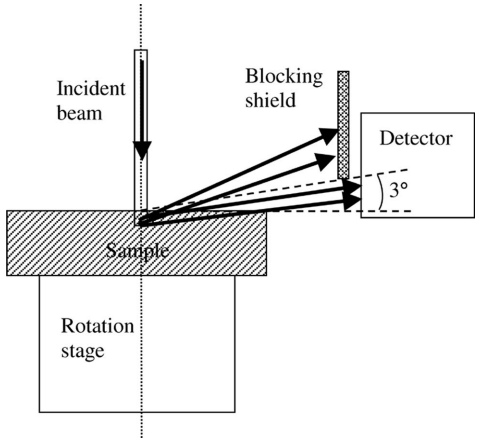

Figure 1
Schematic of the GEA set-up.

Powders were ground to the point of approaching a clay-like consistency and no specular reflection was observed from incident light by optical microscope. Powders were then brushed onto layers of adhesive tape and folded several times in order for the absorption-edge step at the V *K*-edge to be <1. There were no pinholes visible in the final tapes. The incident X-ray beam was detuned by 30% in all cases.

3. Results

Representative XANES data for a single-crystal sample with $x = 0.0285$ for $\mathbf{E}\parallel c$ and $\mathbf{E}\perp c$ are shown in Fig. 2(*a*). After averaging the polarized spectra in accordance with equation (2), the resultant signal was compared with an XANES spectrum measured independently from the powdered sample (Fig. 2*b*). Plots of the EXAFS data for the same sample before and after averaging are shown in Figs. 3 and 4 in *k*-space and *r*-space, respectively.

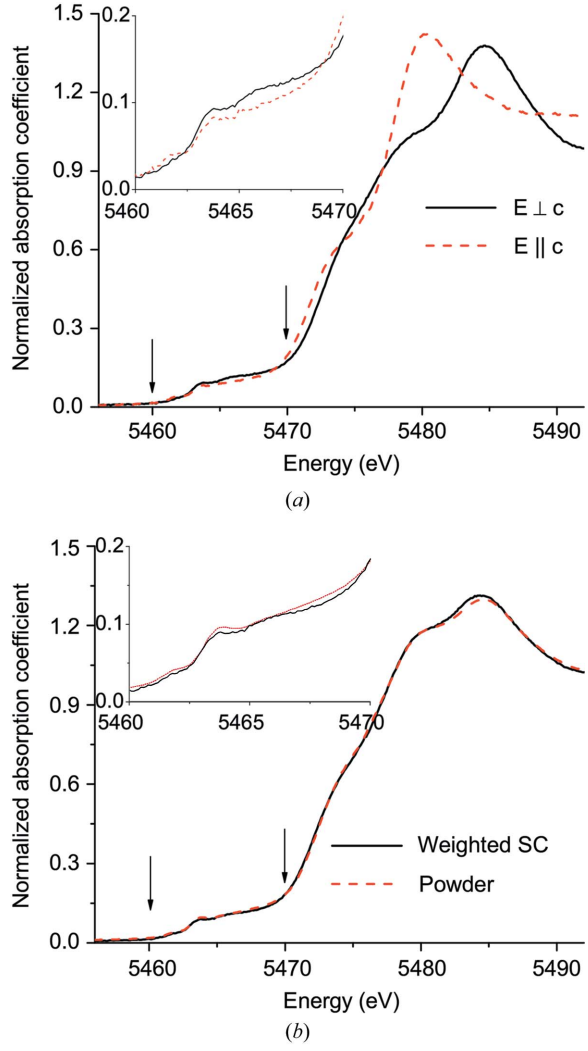

Figure 2
Polarized data for $\mathbf{E}\parallel c$ and $\mathbf{E}\perp c$ for $x = 0.0285$ (*a*). Weighted average of polarized XANES data are shown together with XANES in the powdered sample for the same x (*b*). The inset shows the 1*s*–*d* transition regions, denoted by arrows.

Table 1
Bond lengths (in Å, with error bars shown in parentheses) between V and its nearest neighbors obtained by polarized EXAFS measurements of the V *K*-edge in single crystals (SC) and powders (P) for x = 0, 00116, 00285 and 00523; X-ray diffraction data (XRD) (Dernier & Marezio, 1970) are shown for comparison.

x	V–O SC	V–O P	V–O XRD	V–V(ax) SC	V–V(ax) P	V–V(ax) XRD	V–V(bp) SC	V–V(bp) P	V–V(bp) XRD
0	2.007 (8)	2.009 (6)	2.01	2.71 (3)	2.72 (8)	2.70	2.90 (1)	2.91 (3)	2.88
0.0116	2.00 (2)	2.017 (7)		2.74 (3)	2.8 (4)		2.92 (4)	2.94 (5)	
0.0285	2.00 (2)	2.017 (6)		2.77 (3)	2.81 (14)		2.94 (3)	2.95 (2)	
0.0381			2.018			2.75			2.92
0.0523	2.00 (1)	2.013 (7)		2.76 (3)	2.8 (2)		2.94 (2)	2.94 (2)	

It is evident from Figs. 2–4 that the polarization-averaged single-crystal data and the powder transmission data are in good agreement throughout the entire energy range. As an additional reliability check, we compared the V–O and V–V distances obtained from the powder analysis against those obtained from the polarized EXAFS analysis (Frenkel *et al.*, 2006). The results of both methods agreed within experimental uncertainties (Table 1). However, since there is directional information present in the GEA on single crystals not present for random powders, analysis of the former system is much more valuable for structural studies. Additionally, access to polarized XANES data (Fig. 2*b*, inset) is valuable in its own right: in transition metal compounds the absorption coefficient in the pre-edge region is sensitive to the *d–p* hybridization of the transition metal and surrounding O atoms (Farges *et al.*, 1997; Kraizman *et al.*, 1995; Aguirre-Tostado *et al.*, 2004), and contains a wealth of structural and electronic information for a large variety of materials.

Table 1 shows distance information for V and its nearest neighbors obtained by EXAFS analysis from the single-crystal data (using polarized measurements) and from the powder data. X-ray diffraction data (Dernier & Marezio, 1970; Dernier, 1970) in metal and insulator phases are also given for comparison. Table 1 demonstrates that the results obtained by these techniques for different samples are the same within uncertainties. It is evident, however, that the precision of distance determination is much better in the case of polarized measurements compared with powder ones, with the exception of the V–O distances, which were obtained with similar uncertainties. For V–V distances measured in the axial

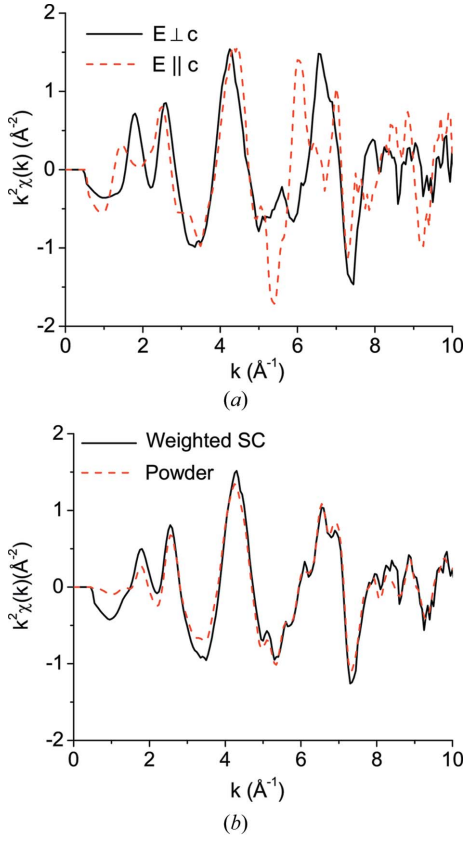

Figure 3
Polarized k^2-weighted $\chi(k)$ data for $\mathbf{E} \parallel c$ and $\mathbf{E} \perp c$ for x = 0.0285 (*a*). EXAFS data in k-space obtained from $\mu_{av}(E)$ and $\mu_{pow}(E)$ (*b*).

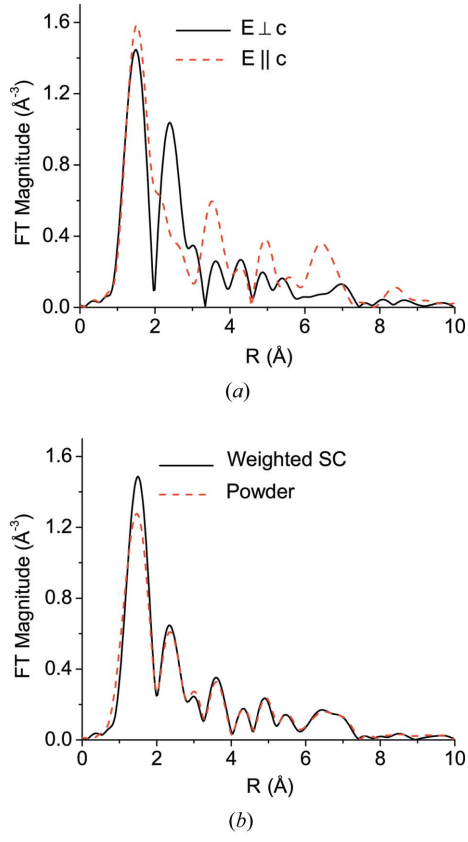

Figure 4
Fourier-transform magnitudes of polarized k^2-weighted $\chi(k)$ data for $\mathbf{E} \parallel c$ and $\mathbf{E} \perp c$ for x = 0.0285 (*a*). EXAFS data in r-space obtained from $\mu_{av}(E)$ and $\mu_{pow}(E)$ (*b*).

[(V–V(ax)] and basal plane [(V–V(bp)] directions, analysis of the polarized EXAFS measurements resulted in much smaller error bars than for the powder analysis. The accuracy in these distances (0.01–0.03 Å for the metallic and insulating phases) achieved with polarized measurements was just sufficient to observe the mismatch (0.06 Å or less) between the V–(V,Cr) and Cr–(V,Cr) distances in the axial and basal plane directions in $(Cr_xV_{1-x})_2O_3$. Measurements taken in the powder would not allow us to make this determination, since the error bars in the V–V distances were as large as 0.05–0.4 Å depending on the concentration (Table 1).

4. Discussion and conclusions

We have demonstrated that the GEA method of the synchrotron X-ray fluorescence mode of XAFS data collection, known previously for effectively suppressing fluorescence distortion in bulk samples, is a powerful method for obtaining orientation-dependent results in single crystals. Comparison with powder transmission data shows that it need not be necessary to use difficult sample preparation techniques such as magnetically orienting powders for transmission experiments, or making samples into thin films, to obtain excellent orientation-dependent results. In the XANES region particularly, the extent to which one can remove fluorescence distortion depends on the limitations on count rate as one goes to increasingly glancing emergent angles. A better method to use than that applied here would be based on the apparatus developed by Brewe *et al.* (1992), in which the emergent beam is detected along essentially half a 360° arc by using a special detector made from PIN diodes. This technique yields a much greater solid angle than the method used here, but the apparatus of Brewe *et al.* does not include a rotation-stage capability necessary for the present application. It would be possible to modify the device developed by Brewe *et al.* to include rotation scans as in the present work. For the present set-up, using a beam limited by the sample size to about half a centimeter at an unfocused standard beamline and second-generation synchrotron, we scanned for a few hours on each sample to obtain good data. Despite the rather long scan times, the GEA method is applicable for measuring not only the EXAFS but also the near-edge (XANES) spectra, which is particularly valuable for materials with overlapping edges and for vast numbers of transition metal compounds where the XANES signal is sensitive to the X-ray polarization direction.

The authors acknowledge support by the US Department of Energy Grant No. DE-FG02-05ER36184. The NSLS is supported by the Divisions of Materials and Chemical Sciences of the US Department of Energy. The authors acknowledge assistance from Kumi Pandya at the NSLS.

References

Aguirre-Tostado, F. S., Herrera-Gomez, A., Woicik, J. C., Droopad, R., Yu, Z., Schlom, D. G., Zschack, P., Karapetrova, E., Pianetta, P. & Hellberg, C. S. (2004). *Phys. Rev. B*, **70**, 201403R.
Booth, C. H. & Bridges, F. (2005). *Phys. Scr.* T**115**, 202–204.
Brewe, D. L., Bouldin, C. E., Pease, D. M., Budnick, J. I. & Tan, Z. (1992). *Rev. Sci. Instrum.* **63**, 3298–3302.
Brewe, D. L., Pease, D. M. & Budnick, J. I. (1994). *Phys. Rev. B*, **50**, 9025–9030.
Dernier, P. D. (1970). *J. Phys. Chem. Solids*, **31**, 2569–2575.
Dernier, P. D. & Marezio, M. (1970). *Phys. Rev. B*, **2**, 3771–3776.
Farges, F. G., Brown, E. & Rehr, J. J. (1997). *Phys. Rev. B*, **56**, 1809–1819.
Frenkel, A. I., Pease, D. M., Budnick, J., Metcalf, P., Stern, E. A., Shanthakumar, P. & Huang, T. (2006). *Phys. Rev. Lett.* **97**, 195502.
Frenkel, A. I., Stern, E. A. & Chudnovsky, F. A. (1997). *Solid State Commun.* **102**, 637–641.
Goulon, J., Goulon-Ginet, C., Cortes, R. & Dubois, J. M. (1982). *J. Phys. (France)*, **43**, 539–543.
Haskel, D., Stern, E. A., Dogan, F. & Moodenbaugh, A. (2000). *Phys. Rev. B*, **61**, 7055–7076.
Haskel, D., Stern, E. A., Hinks, D. G., Mitchell, A. W., Jorgensen, J. & Budnick, J. (1996). *Phys. Rev. Lett.* **76**, 439–442.
Kraizman, V. L., Novakovich, A. A., Vedrinskii, R. V. & Timoshevskii, V. A. (1995). *Physica B*, **209**, 35–36.
Kuykendall, T., Pauzauskie, P. J., Zhang, Y., Goldberger, J., Sirbuly, D., Denlinger, J. & Yang, P. (2004). *Nature Mater.* **3**, 524–528.
McWhan, D. B. & Remeika, J. P. (1970). *Phys. Rev. B*, **2**, 3734–3750.
Metcalf, P. & Honig, J. (1995). *Curr. Topics Cryst. Growth Res.* **2**, 445–455.
Nelson, E. J., Woicik, J. C., Hong, M., Kwo, J. & Mannaerts, J. P. (2000). *Appl. Phys. Lett.* **76**, 2526–2528.
Newville, M. (2001). *J. Synchrotron Rad.* **8**, 322–324.
Pease, D. M., Brewe, D. L., Tan, Z., Budnick, J. I. & Law, C. C. (1989). *Phys. Lett. A*, **138**, 230–234.
Pfalzer, P., Urbach, J. P., Klemm, M., Horn, S., den Boer, M. L., Frenkel, A. & Kirkland, J. P. (1999). *Phys. Rev. B*, **60**, 9335–9339.
Suzuki, Y. (1989). *Phys. Rev. B*, **39**, 3393–3395.
Tan, Z., Budnick, J. I. & Heald, S. M. (1981). *Rev. Sci. Instrum.* **60**, 1021–1025.
Tranquada, J. M., Heald, S. M., Moodenbaugh, A. & Suenaga, M. (1987). *Phys. Rev. B*, **35**, 7187–7190.
Tröger, L., Arvanitis, D., Baberschke, K., Michaels, H., Grimm, U. & Zschech, E. (1992). *Phys. Rev. B*, **46**, 3283–3289.
Woicik, J. C., Bouldin, C. E., Miyano, K. E. & King, C. A. (1997). *Phys. Rev. B*, **55**, 15386–15389.